ELSEVIER

Surface Science 331-33 (1995) 1372-1376

surface science

Electric field dynamics at a metal–semiconductor interface probed by femtosecond optical second harmonic generation

W. de Jong [a], A.F. van Etteger [a], C.A. van 't Hof [a], P.J. van Hall [b], Th. Rasing [a,*]

[a] *Research Institute for Materials, Toernooiveld, 6525 ED Nijmegen, Netherlands*

[b] *Department of Physics, Eindhoven University of Technology, P.O. Box 513, 5600 MB Eindhoven, Netherlands*

Received 29 August 1994; accepted for publication 25 November 1994

Abstract

The optical second harmonic generation (SHG) from a Au/GaAs(100) Schottky barrier is shown to be a direct probe of the electric field dynamics near such a metal–semiconductor interface. The variation of the field induced SHG amplitude with the power and pulse width of the femtosecond excitation is found to be in good agreement with Monte Carlo simulations.

Keywords: Gallium arsenide; Schottky barrier; Second Harmonic Generation; Surface electrical transport

1. Introduction

The problem of Schottky barrier formation at a metal–semiconductor interface still attracts a lot of attention, as new developments in material fabrication and structure determination have shown that the precise interface structure plays a crucial role in determining the Schottky barrier height [1,2]. For electro-optic applications, not only the static electronic structure but even more importantly, the dynamics near these barriers is extremely relevant, as this will affect the speed of such devices. Recent photoluminescence studies of ultrafast carrier dynamics at a metal–semiconductor interface have shown unexpected field and laser intensity dependences [3]. Theoretical models suggest a very rapid drop and possible oscillation of the internal electric field at the metal–semiconductor interface as a result of the spatial separation of the carriers excited by the incident laser pulse [4]. These observations are very interesting and important as they happen already at quite moderate laser powers (~10 mW), commonly used in optical semiconducting devices. However, the photoluminescence signal is only very indirectly affected by the internal field, and the results depend on line shape analysis and deconvolutions.

SHG in reflection from centrosymmetric semiconductor surfaces and interfaces has already been shown to be an effective method of probing the structure and symmetry of interface layers [5–10]. The surface/interface sensitivity in those situations is based on the symmetry breaking at interfaces and the SHG-intensity is found to be strongly dependent on surface orientation, defect generation, adsorption, and so on. Very recently, Qi et al. [11] showed the capability of SHG to probe the bandbending region of GaAs, using a tunable excitation source. Lantz et al. [12] used SHG to probe the electrostatic fields at TiO_2 electrodes. An advantage of such an optical method is the possibility of probing buried interfaces, such as a transparant metal gate–semiconductor interface.

* Corresponding author. Fax: +31 80 652190; E-mail: theoras@sci.kun.nl.

0039-6028/95/$09.50
SSDI 0039-6028(95)00397-7

In this paper we present the first results of a femtosecond SHG study of the electric field dynamics near a Schottky barrier interface, formed by a thin Au layer on top of GaAs(100). Measurement of the azimuthal SHG anisotropy in the presence of a reverse bias allows a clear separation of bulk contributions and bias field induced interface contributions. The results show a clear bias dependence, that is suppressed at higher incident laser powers. To probe the time dependence of this interface contribution we vary the width of the femtosecond excitation pulse. The rate of the suppression appears to depend on this pulse width. The field-induced SHG thus gives a direct probe of the field dynamics near a Schottky barrier interface. Similar dynamics studies on a semiconductor surface have been reported by Dekorsy et al. [13], employing an ultrafast linear electro-optic technique.

2. Theory

For an incident electric field $E(\omega)$ the SHG-field follows from the nonlinear polarization $P(2\omega)$. In the electric dipole approximation $P(2\omega)$ is related to $E(\omega)$ and a DC electric field $E_{SB}(0)$ via nonlinear susceptibility tensors as:

$$P(2\omega) = \left(\chi_I^{(2)} + \chi_B^{(2)}\right) : E(\omega)E(\omega) + \left(\chi_I^{(3)} + \chi_B^{(3)}\right) \vdots E(\omega)E(\omega)E_{SB}(0), \quad (1)$$

where χ_I and χ_B are the interface and bulk nonlinear susceptibility tensors, respectively. Since GaAs does not have inversion symmetry there are both bulk and interface nonzero tensor elements. The GaAs(100) surface has 4 mm symmetry and the three independent non-zero interface susceptibility elements are $\chi_{I;zzz}^{(2)}$, $\chi_{I;zii}^{(2)}$ and $\chi_{I;izi}^{(2)}$ with $i = x, y$ [14,15]. For the bulk of the 43 m symmetric GaAs(100) crystal there is only one independent non-zero susceptibility element $\chi_B^{(2)} = \chi_{B;ijk}^{(2)}$ with $i \neq j \neq k$ [15]. The subscripts (i, j, k) refer to the principal axes (x, y, z) of the cubic crystal, with z along the interface normal. The second term in Eq. (1) describes the so called electric field induced second harmonic generation. The DC field $E_{SB}(0)$ has only a z-component, which we will indicate with E_{SB}. After multiplication with E_{SB} the fourth rank tensors in the second term of Eq. (1) reduce to third rank tensors having the same non-zero elements as the tensors $\chi_I^{(2)}$ and $\chi_B^{(2)}$ [8,11].

The p-component of the SHG intensity $I_{2\omega}$ reflected from the sample is measured for a p-polarized pump beam. This $I_{2\omega}$ is proportional to $|E_{pp}(2\omega)|^2$ and $E_{pp}(2\omega)$ is proportional to the nonlinear polarization $P(2\omega)$. Using the bulk and interface tensor elements $E_{pp}(2\omega)$ is given by Refs. [15,16]:

$$E_{pp}(2\omega) \sim f_I \left(\chi_I^{(2)} + \chi_{I;z}^{(3)} E_{SB}\right) |E(\omega)|^2 + f_B L \cos 2\psi \left(\chi_B^{(2)} + \chi_{B;z}^{(3)} E_{SB}\right) |E(\omega)|^2. \quad (2)$$

Here f_I and f_B denote the appropriate Fresnel coefficients, which depend on the dielectric constants of GaAs at the photon energies involved and the angle of incidence. ψ denotes the angle between the (100) direction and the plane of incidence. For the bulk contributions the coefficient L represents the effective phase matching distance in the crystal. From Eq. (2) it follows that for the p-in, p-out polarization combination the bulk contribution to $I_{2\omega}$ gives a fourfold anisotropy when the GaAs(100) crystal is rotated around its interface normal, while the interface contribution is isotropic. This offers a possibility to separate the bulk and interface contributions to $I_{2\omega}$.

3. Experiment

The Schottky barrier sample we used for our experiments, is grown on an n^+ GaAs substrate. The actual barrier is formed by a 0.3 μm-thick n-type GaAs (doping concentration: 10^{17} cm^{-3}) layer and a semi-transparant Gold film of 80 Å thickness, to allow for laser excitation through the metal top contact. To suppress interface recombination and provide for a superior optical quality the sample contains a very thin (100 Å) intermediate undoped $Al_{.4}Ga_{.6}As$-layer between the metal and the depletion layer, capped by a 100 Å thick undoped GaAs-layer, as well as a heavily doped n-type (doping concentration: 10^{18} cm^{-3}) superlattice buffer layer (100×50 Å GaAs/50 Å $Al_{.33}Ga_{.67}As$) between the depletion layer and the n^+-GaAs substrate. A voltage bias can be applied across the sample between a AuGeNi backside-contact and the top contact. Capacitance–voltage measurements indicate a value for the Schottky barrier height of 0.90 V.

For the SHG measurements we used a mode-locked Titanium Sapphire laser that operated at λ = 770 nm and produced trains of 70 fs pulses at a 82 MHz repetition rate. The photon energy at this wavelength is 1.61 eV; this is above the bandgap of GaAs. The sample was subjected to radiation at a 45° angle of incidence. The diameter of the spot was about 100 μm. We measured $I_{2\omega}$ versus the rotation angle ψ of the sample, the so called azimuthal anisotropy, for different reversed-bias voltages, different laserpowers, and different values of the pulse width. For these measurements a stepping motor rotator is used, and extreme care was taken to keep the alignment of the sample constant while rotating or changing the bias voltage and the laserpower. To compress the pulses we used pairs of prisms as described by Fork et al. [17]. To get longer pulses, the pulses were stretched with an Amici-prism.

4. Results and discussion

Fig. 1a shows half of the azimuthal anisotropy for two different bias voltages, measured with a pulse width of 221 fs and an average laser power of 5.5 mW. Fig. 1b shows the same, measured with an average laser power of 17.5 mW. The open circles present data at 0 V bias, the dots at −4 V. In Fig. 1a a very clear bias dependence of $I_{2\omega}$ can be seen, that practically disappears for 17.5 mW excitation as shown in Fig. 1b.

This kind of measurement was done for different pump-power values ranging from 3 to 19 mW average pump-power, and with three different pulse widths, 42 fs, 114 fs and 221 fs. The reversed bias voltage is changed from 0 V to −4 V.

According to Eq. (2) the $I_{2\omega}$ can be described by:

$$I_{2\omega} = |A_{\rm I} \exp({\rm i}\phi) + A_{\rm B} \cos 2\psi|^2. \qquad (3)$$

The measured curves are fit to Eq. (3) with the following three fitting parameters: the interface amplitude $A_{\rm I}$, the phase angle ϕ and the bulk amplitude $A_{\rm B}$. With Eq. (3) we were able to fit the experimental data very well as is shown by the solid lines in Fig. 1.

The amplitude of the bulk contribution $A_{\rm B}$ is inversely proportional to the square root of the pulsewidth of the laserpulses and depends linearly

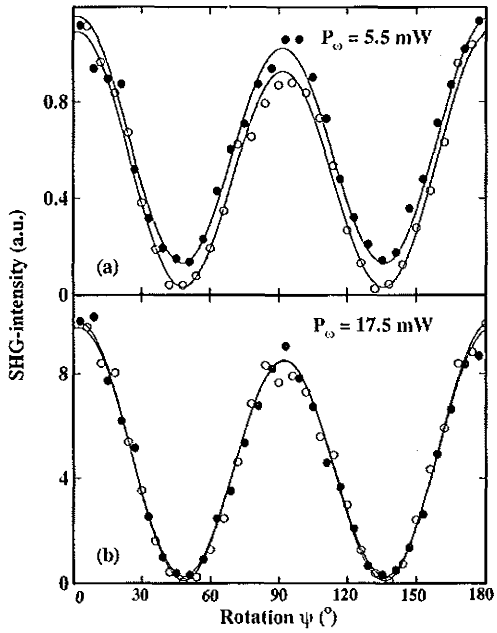

Fig. 1. (a) Azimuthal anisotropy of the GaAs/Au sample for two different bias voltages, measured with an average laser power of 5.5 mW and pulse width of 221 fs. The open circles present data at 0 V bias, the dots at −4 V. The lines are a fit, according to formula (3). (b) The same, but measured with an average laser power of 17.5 mW.

on the average pump-power, which is directly proportional to $|E(\omega)|^2$. This is the expected behaviour of bulk SHG [14]. The bulk contribution appears to be insensitive to changes in the applied bias voltage. $A_{\rm B}$ only decreases by a few percent when the reversed bias voltage is changed from 0 V to −4 V. This means that $\chi_{\rm B}^{(2)}$ from Eq. (2) is independent of the bias voltage or pump power, and that $\chi_{\rm B;z}^{(3)}$ equals zero. The interface amplitude $A_{\rm I}$ is normalised to $A_{\rm B}$. Since $A_{\rm B}$ is directly proportional to $|E(\omega)|^2$ and $\chi_{\rm B}^{(2)}$ is a constant, this gives for the normalised interface contribution $A_{\rm I}'$:

$$A_{\rm I}' \sim |\chi_{\rm I}^{(2)} + \chi_{\rm I;z}^{(3)} E_{\rm SB}|. \qquad (4)$$

The maximum static electric field $E_{\rm SB}$ at the SB interface is calculated from the well known equation [18]

$$|E_{\rm SB}| = \left(\frac{2qN_{\rm D}\Phi_{\rm b}}{\epsilon_0 \epsilon_{\rm S}}\right)^{1/2}, \qquad (5)$$

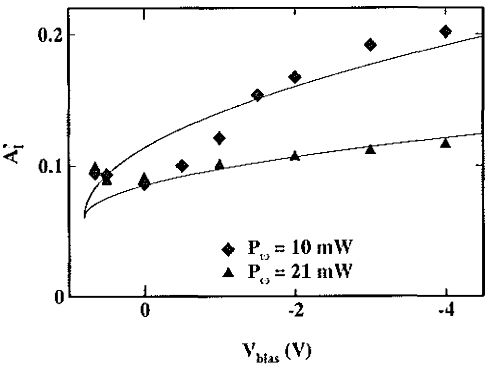

Fig. 2. Bias dependence of the normalised interface contribution measured with a pulsewidth of 42 fs at two different values of the average laser power P_ω, 10 and 21 mW. The lines are a fit, according to formula (6).

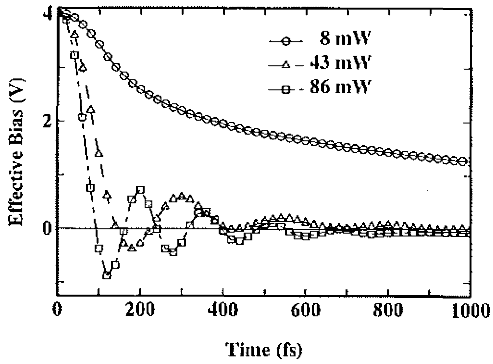

Fig. 3. Time evolution of the effective bias voltage, calculated for an initial bias voltage of −4 V and a regeneration time of 10 ps for a number of input powers (legends correspond to input power).

where N_D is the doping density, ϵ_0 is the dielectric permittivity, ϵ_S is the static dielectric constant, and Φ_b is the bandbending at the interface. The latter is given by: $\Phi_b = \Phi_{b0} + V_b$, where Φ_{b0} is the bandbending when no biasvoltage is applied and V_b is the absolute value of an applied reversed bias voltage.

From Eqs. (4) and (5) we expect A_I' as a function of V_b to be of the following form:

$$A_I' = C_0 + C_I\sqrt{\Phi_{b0} - V_b}. \quad (6)$$

Fig. 2 shows the bias dependence of A_I' measured with a pulse width of 42 fs at two different values of the average laser power P_ω, 10 and 21 mW. The lines are a fit, according to formula (6) with C_0 and C_I as fitting parameters. Using formulas from Sze [18] Φ_{b0} is calculated to be equal to 0.8 V. With $C_0 = 0.06$ the fit is in good agreement with our results. C_I depends on the average power of the incident laser beam. This agreement indicates that the isotropic component is indeed generated at the metal–semiconductor interface.

The pump laser beam will not only generate SH but it also excites charge carriers since the photon energy is above the bandgap of GaAs. In a reversely biased Schottky barrier these carriers will move away from each other due to the internal depletion electric field. The resulting charge separation will cause an almost instantaneous collapse of this field, that will only recover after some time. This means that for short optical pulses the effective bias field can be very different from the initial applied one, depending on the intensity used. Monte Carlo simulations were performed to calculate the time dependence of the electric field for different values of the laser intensity. The device is modeled schematically as described previously [4]. The 0.3 μm-thick GaAs layer is separated from the Au by a barrier formed by the intermediate AlGaAs layer and the Schottky barrier. The applied bias voltage creates an interface charge at the Au film which is compensated for by a constant intrinsic space-charge throughout the whole depletion layer giving rise to a linearly decreasing electric field and a parabolic potential. Due to its heavy doping the superlattice is assumed to form no barrier for the electrons and a large one for the holes.

An important point to note is the following. Very shortly after excitation a number of holes will reach the top Au contact, where they neutralize the surface charge, leading to a reduced field strength. In the case that the photo-excited charge density exceeds significantly the intrinsic one, the applied field may be quenched totally by only a small part of the excited holes. A similar effect occurs when the holes are collected in front of the AlGaAs barrier where they screen the applied voltage. It will take some time before the field will be restored. Based on the capacitance per area (520 $\mu F/m^2$), the size of the excitation beam (100 μm) and the square resistance of the Au film (a few Ohms), we estimated the RC time constant of this process to be in order of 10 ps.

The subsequent transport and energy relaxation of the photo-excited carriers in the GaAs layer are computed in a Monte Carlo simulation, accounting for the various scattering mechanisms. Both electron-heavy

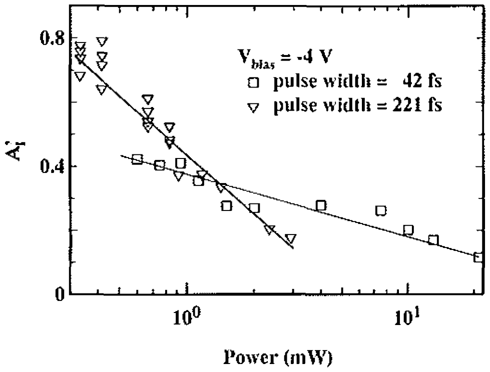

Fig. 4. Power dependence of the normalised interface contribution A_S^f measured at −4 V bias with a pulsewidth of 221 fs and 42 fs. The lines are to guide the eye.

and electron-light hole pairs are considered, including hole inter-band transitions. We used a Gaussian pulse width for the exciting laser pulse.

Obviously the photo-excitation gives rise to a space-charge field. Directly after excitation, when the electrons and holes are still close to each other this field is zero. However, as soon as the electrons and holes start to move as a result of the applied field, a counteracting electric field will be build up. To account for this space-charge effect the Poisson equation has been solved in one dimension every 1 fs of the calculation. Fig. 3 depicts the calculated time evolution of the effective bias for an initial bias voltage of −4 V using a regeneration time of 10 ps.

In Fig. 4 the power dependence of A_I^f measured at −4 V bias and with pulsewidths of 42 fs and 221 fs is plotted. This figure shows that A_I^f decreases as the average laser power is increased. This is expected for the effective bias as can be seen in Fig. 3. In the experiment one laser pulse generates the carriers and also probes the field by generating the electric field induced SHG signal. So the time resolution of the 'probe' is of the order of the pulse width. The decrease of A_I^f in Fig. 4 is more drastic for 221 fs pulses than for the 42 fs ones, indicating that for very short pulses, the system is still close to the initial situation. This is in agreement with the simulation in Fig. 3.

5. Conclusion

In conclusion, we have shown that second harmonic generation in reflection is a useful tool to probe the electric field at a metal-semiconductor interface. By selecting the proper polarization combinations the interface and bulk contributions to the SHG signal of a Au/GaAs(100) Schottky barrier are easily separated. It appears that the bulk second order susceptibility is independent of the bias voltage or the laser intensity. The normalised interface contribution appears to be proportional to the static electric field at the Schottky barrier interface. The power dependence of A_S^f is in qualitative agreement with Monte Carlo simulations. Future work is to measure the electric field dynamics with a time-resolved pump-probe technique.

References

[1] D.R. Heslinga, H.H. Weitering, D.P. van der Werf, T.M. Klapwijk and T. Hibma, Phys. Rev. Lett. 64 (1990) 1589.
[2] S. Chang, L.J. Brillson, Y.J. Kime, D.S. Rioux, P.D. Kirchner, G.D. Pettit and J.M. Woodall, Phys. Rev. Lett. 64 (1990) 2551.
[3] P.C.M. Christianen, PhD thesis, University of Nijmegen (1993).
[4] P.C.M. Christianen, P.J. van Hall, H.J.A. Bluyssen and J.H. Wolter, Semicond. Sci. Technol. 9 (1994) 707.
[5] Y.R. Shen, Nature 337 (1989) 519.
[6] G.L. Richmond, J.M. Robinson and V.L. Shannon, Prog. Surf. Sci. 28 (1988) 1.
[7] H.W.K. Tom, T.F. Heinz and Y.R. Shen, Phys. Rev. Lett. 51 (1983) 1983.
[8] S.V. Govorkov, V.I. Emel'yanov, N.I. Koroteev, G.I. Petrov, I.L. Shumay and V.V. Yakovlev, J. Opt. Soc. Am. B 6 (1989) 1117.
[9] C.W. van Hasselt, M.A. Verheijen and Th. Rasing, Surf. Sci. 251 (1991) 467.
[10] G.G. Malliaras, H.A. Wierenga and Th. Rasing, Surf. Sci. 287 (1993) 703.
[11] J. Qi, M.S. Yeganeh, I. Koltover, A.G. Yodh and W.M. Theis, Phys. Rev. Lett. 71 (1993) 633.
[12] J.M. Lantz and R.M. Corn, J. Phys. Chem. 98 (1994) 4899.
[13] T. Dekorsy, T. Pfeifer, W. Kütt and H. Kurz, Phys. Rev. B 47 (1993) 3842.
[14] Y.R. Shen, The Principles of Nonlinear Optics (Wiley, New York, 1984).
[15] T. Stehlin, M. Feller, P. Guyot-Sionnest and Y.R. Shen, Opt. Lett. 13 (1988) 389.
[16] R.W.J. Hollering, Opt. Commun. 90 (1992) 147.
[17] R.L. Fork, O.E. Martinez and J.P. Gordon, Opt. Lett. 9 (1984) 150.
[18] S.M. Sze, Physics of Semiconductor Devices, 2nd ed. (Wiley, New York, 1981).